Glycobiology vol. 24 no. 8 pp. 703–714, 2014
doi:10.1093/glycob/cwu034
Advance Access publication on May 2, 2014

O-Linked glycosylation in *Acanthamoeba polyphaga* mimivirus

Andreas J Hülsmeier[1] and Thierry Hennet

Institute of Physiology, University of Zurich, Winterthurerstrasse 190, Zurich 8057, Switzerland

Received on December 18, 2013; revised on April 24, 2014; accepted on April 24, 2014

***Acanthamoeba polyphaga* mimivirus is a member of the giant nucleocytoplasmic large DNA viruses, infecting various *Acanthamoeba* spp. The genomes of giant viruses encode components previously thought to be exclusive to cellular life, such as proteins involved in nucleic acid and protein synthesis. Recent work on enzymes involved in carbohydrate biosynthesis and metabolism show that instead of utilizing host cell resources, Mimivirus produces its own glycosylation machinery. To obtain a more detailed view of glycosylation in Mimivirus, we developed a periodate oxidation-based method to selectively enrich Mimivirus surface glycoproteins. O-Glycosylation in Mimivirus glycoproteins was identified by permethylation and matrix-assisted laser desorption/ionization-mass spectrometry analyses of beta-eliminated glycans. We sequenced 26 previously undescribed O-glycans, most of which contain glucose as their reducing end saccharide. These data will facilitate future studies on the functional significance of glycosylation in Mimivirus.**

Keywords: beta-elimination / glycoprotein enrichment / MALDI-mass spectrometry / methylation / reducing-end analysis

Introduction

Acanthamoeba polyphaga mimivirus (Mimivirus) belongs to the nucleocytoplasmic large DNA viruses (NCLDVs) which includes *Phycodnaviridae*, *Poxviridae*, *Asfarviridae*, *Iridoviridae*, *Ascoviridae*, *Mimiviridae* and *Marseilleviridae* (Van Etten, Lane, et al. 2010). A recent addition to the new family of giant viruses describes the largest viral genomes and the genus name Pandoravirus was proposed (Philippe et al. 2013). Mimivirus was the first member of the giant viruses to be described, and gave its name to the family *Mimiviridae*. NCLDVs contain internal lipid bilayer membranes and the some *Iridoviridae* and *Mimiviridae* can be covered by long fibers protruding from the outer surface of their capsids (Yan et al. 2000; Xiao et al. 2005). NCLDVs display characteristics previously thought to be exclusive to cellular life. Their genes encode proteins involved in DNA repair, RNA translation and protein synthesis (Claverie and Abergel 2009). Members of the family *Phycodnaviridae* infect algae and *Mimiviridae*, the largest members of NCLDVs by particle and genome size, infect amoebae found in both fresh and salt water environments (Wilson et al. 2009; Thomas et al. 2011; Boughalmi et al. 2013). The 1.2 Mb genome of Mimivirus has been sequenced and contains 1018 genes with 979 open-reading frames annotated to code for proteins (Raoult et al. 2004; Legendre et al. 2011).

Mimivirus encodes its own glycosylation machinery, a characteristic that also has been reported for a member of the *Phycodnaviridae* family, *Paramecium bursaria* chlorella virus. The glycosylation machinery of *P. bursaria* chlorella virus has been described to modify viral proteins independent of the host ER or Golgi apparatus. *Paramecium bursaria* chlorella virus encodes at least five glycosyltransferases as well as other enzymes involved in carbohydrate metabolism (Van Etten, Gurnon, et al. 2010). Its major capsid protein Vp54 is N-glycosylated at four Asn and O-glycosylated at two Ser sites as revealed by crystal structural analysis (Nandhagopal et al. 2002). The chemical structure of four highly branched and unusual Vp54 N-glycoforms was reported recently (De Castro et al. 2013). The first indications of glycosylation in Mimivirus came from its Gram-positive staining and the detection of protein isoforms by 2D polyacrylamide gel electrophoresis (PAGE) (Raoult et al. 2004). Furthermore, carbohydrate-targeted gel-staining assays indicated the presence of various glycoproteins in Mimivirus extracts (Raoult et al. 2004; Renesto et al. 2006; Boyer et al. 2011). The Mimivirus fibers appear to be particularly rich in carbohydrate modification, as indicated by comparing the sugar compositions of intact versus de-fibered viral particles (Piacente et al. 2012). Analysis of the Mimivirus genome predicted the presence of six glycosyltransferase genes in addition to enzymes required for the biosynthesis of UDP-L-rhamnose and unusual amino-sugars such as viosamine (4-amino-4,6-dideoxy-D-glucose, Vio) (Raoult et al. 2004; Parakkottil Chothi et al. 2010; Piacente et al. 2012). The first Mimivirus glycosyltransferase has been characterized recently, and shown to be a bi-functional enzyme capable of hydroxylating lysine and transferring glucose (Glc) to collagen substrates (Luther et al. 2011).

Although the presence of glycosylation in Mimivirus is well established, the extent and nature of Mimivirus glycosylation

[1]To whom correspondence should be addressed: Tel: +41-44-635-5104; Fax: +41-44-635-6814; e-mail: a.j.hulsmeier@access.uzh.ch

remains incompletely understood. Nothing is known about N-linked and O-linked glycosylation in Mimivirus, and only a few glycoproteins have been detected by an in-gel fluorescence staining approach using a no longer available commercial kit (Renesto et al. 2006; Boyer et al. 2011). A more detailed understanding of Mimivirus surface glycosylation will foster future studies on Mimivirus biology, such as those addressing the role of glycosylation in virus–host interactions.

Results

With little known about glycosylation in Mimivirus, we aimed to first identify Mimivirus glycoproteins. Based on carbohydrate periodate oxidation we developed a method to selectively enrich glycoproteins from the viral surface. We then released and examined a diverse spectrum of linear and branched Mimivirus O-glycans. In terms of total amount most glycans contained Glc at their reducing terminus. Further, we addressed the functional significance of Mimivirus surface glycans for the infection of the amoebal host.

Glycoprotein detection

For Mimivirus glycoprotein detection, we employed a biotinylation approach based on periodate oxidation of surface-exposed glycans. Biotin was covalently coupled to oxidized glycans on the virus particles using the aniline-catalyzed transimination reaction with an amino-oxi-biotin probe (Dirksen et al. 2006). To differentiate between specific protein binding to avidin via the biotin probe and unspecific interactions of Mimivirus proteins with the avidin column, we labeled peptides generated from periodate oxidized, biotinylated column eluates versus untreated samples using the 4-plex iTRAQ label reagents. The peptides were subjected to LC-MS sequencing, analyzed and quantified using Mascot and Scaffold Q+ software. The relative enrichment of biotinylated proteins over unreacted proteins was statistically validated using Student's *t*-test and the calculated significance levels for enrichment was plotted against the $\log_2$ value for each detected Mimivirus protein (Figure 1).

Protein enrichments above 1-fold were observed with significance levels of 0.5–1.0 for 40 proteins. High confidence values with significance levels above 0.8, ranging from 1.1-fold up to 3.8-fold enrichments were observed for 28 biotinylated glycoproteins. The relatively broad range of fold enrichments may reflect relative differences in glycoprotein abundance. It may also be due to a differential degree of glycan oxidation with periodate, depending on the number of saccharides containing *cis*-hydroxyl versus *trans*-hydroxyl configurations (Honeyman and Shaw 1959). Low enrichments with high significance values reflect the degree of nonspecific binding of Mimivirus proteins to the avidin cartridge. More than half of these enriched surface glycoproteins were also previously detected by surface biotinylation analysis. The majority of these proteins are annotated as uncharacterized proteins in UniProt (Supplementary data Table I). Nevertheless, the crystal structure of the Mimivirus sulfhydryl oxidase R596 was solved previously (Hakim et al. 2012). We showed that this enzyme is located at the viral surface (Shah et al. 2014). Here we could enrich R596 after periodate oxidation/biotinylation, indicating that R596 is a glycoprotein. The significance level for enrichment of 0.73 however, is only moderate (Supplementary data Table I). Further, the virus surface location of collagen-like protein L71 and the thioredoxin domain-containing protein R362 were also described elsewhere (Shah et al. 2014). Both proteins were susceptible to periodate oxidation/biotinylation. Using the avidin cartridge purification, they were enriched 1.4- and 2.1-fold, with high statistical significance (significance level of 0.95 and 1.00). Renesto *et al.* described the Mimivirus

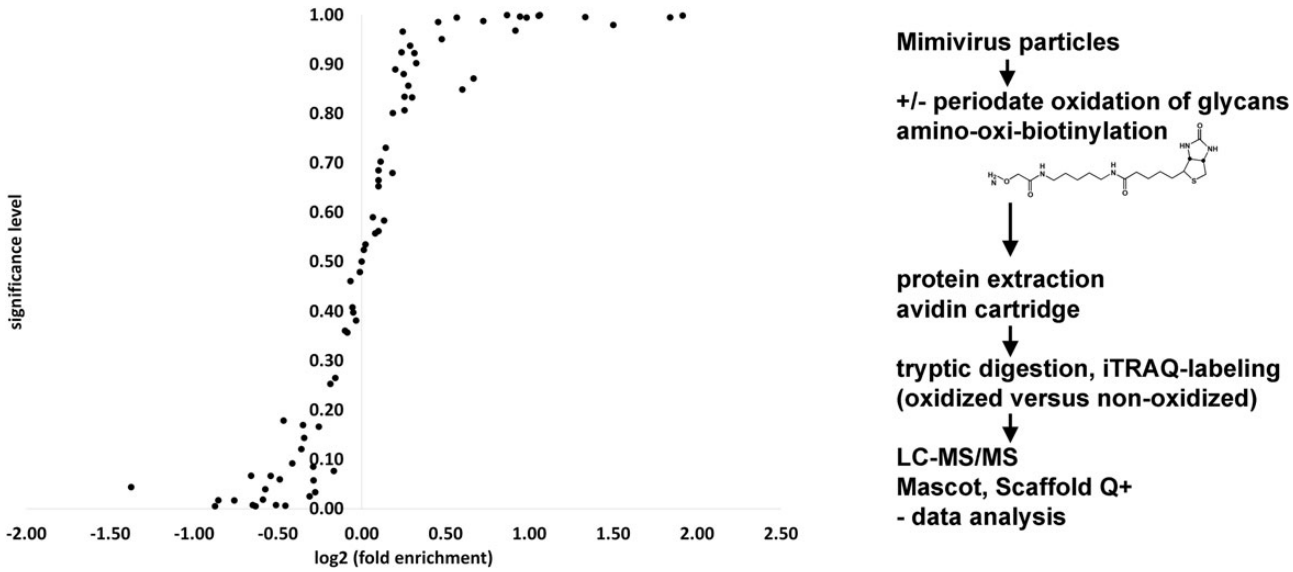

Fig. 1. Enrichment of Mimivirus surface glycoproteins. Log_2 enrichment of oxidized and biotinylated surface-glycoproteins relative to nonoxidized virus particles via avidin cartridge purification. A total of three independent particle oxidation/biotinylation reactions were performed and subjected to avidin cartridge purification. Eluted proteins were subjected to iTRAQ labeling, resulting in nine sample-blank iTRAQ pairs and subjected to mass-spectrometric peptide sequencing. The significance levels for enrichment of oxidized relative to nonoxidized samples were calculated using Student's *t*-test function.

capsid protein L425 as a glycoprotein, using a fluorescent staining protocol for 2D-PAGE (Renesto et al. 2006). We could identify this protein as located at the viral surface (Shah et al. 2014). Nevertheless, in this study, we were unable to confirm L425 as a glycoprotein. Using the periodate-oxidation/biotinylation approach, L425 was only weakly enriched with poor statistical significance (significance level of 0.59, Supplementary data Table I). Using the same 2D-electrophoresis-based glycoprotein staining approach, two further proteins, L829 and L135, were described as glycoproteins of Mimivirus fiber structures (Boyer et al. 2011). Here we could confirm the surface-glycoprotein status for L135 with a significance level of 0.94 (Supplementary data Table I).

Monosaccharide analyses

The monosaccharide constituents in the viral protein extracts were determined by high-performance anion-exchange chromatography with pulsed amperometric detection (HPAEC-PAD) after acid hydrolysis. In Mimivirus samples, three major monosaccharides were detected: rhamnose (Rha), glucosamine (GlcN) and Glc, with a molar ratio of 1.9:2.6:1 (Figure 2). In sample preparations omitting viral particles, the internal standard (Gal) was the only detectable saccharide, indicating that the monosaccharide analyses were unaffected by contaminating sugars.

Small amounts of fucose (Fuc) and Xyl could also be detected. These findings are in good agreement with previous compositional data using gas chromatography coupled mass spectrometry (Piacente et al. 2012). In addition to Rha, GlcN and Glc, Piacente *et al.* also detected Vio, methyl-Vio and minor amounts of mannose (Man) and Gal. We were unable to determine significant amounts of Vio in the Mimivirus protein extracts. Nevertheless, we consistently observed a peak eluting close to the elution position of Vio in the chromatogram (Figure 2). It is tempting to speculate that this peak corresponds to methyl-Vio. With no methyl-Vio standards available

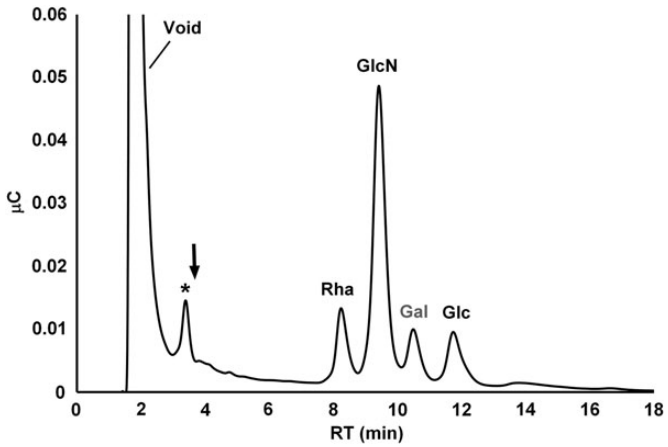

Fig. 2. Monosaccharide analysis of Mimivirus proteins. Protein extract was subjected to acid hydrolysis and the monosaccharides were chromatographed by HPAEC-PAD. The PAD response was measured in Coulomb (µC) and plotted versus the RT. Gal was used as internal standard for quantitation of the monosaccharide constituents. The arrow indicates the elution position of Vio. Asterisk denotes an unidentified peak.

however, we could make no determination for this compound in the current study. We also observed Gal and Man in Mimivirus preparations. After repeated washing of the viral particles however, these saccharides remained below the detection limit of the HPAEC-PAD. Thus, Gal and Man detected in our virus samples probably originated from *Acanthamoeba* used for culturing Mimivirus. Consequently, we used the absence of Gal in the sample preparations as a quality control measure for the purity of the viral particles and for quantitation of monosaccharides, Gal was used as an internal standard.

Reductive β-elimination of Mimivirus O-glycans and reducing-end analyses

The β-elimination reaction releases glycans O-linked to Ser or Thr residues, whereas glycans attached to hydroxylysine are stable to alkaline treatments (Hülsmeier et al. 2011; Luther et al. 2011). Mimivirus O-glycans were radiolabelled by reductive β-elimination from protein extracts in the presence of NaB^3H_4. The released glycans were subjected to HPAEC, using a CarboPac PA200 column. The majority of the radiolabel interacted only weakly with the column and eluted at or near the void volume. The reason for this chromatographic behavior is not clear. Possibly, hydrophobic glycan substitutions are responsible for weak retention on this column and HPAEC may be less suitable for those particular saccharides. Nevertheless, a distinct peak eluting close to the elution position of Glc_4 at 12 min could be observed (Figure 3A).

For determination of the reducing-end saccharide, unfractionated O-glycans, early-eluting and peak fractions at 12 min were subjected to acid hydrolysis and to alditol analysis using a CarboPac MA1 column. Glucitol was the major detected peak in all fractions analyzed, indicating that Glc is a reducing end saccharide in the Mimivirus O-glycan preparation (Figure 3B). Further, we analyzed partially permethylated and perdeuteromethylated alditol acetates (PMAAs) prepared from Mimivirus O-glycans by gas chromatography mass spectrometry (GC-MS). We identified 2-, 6-substituted Glc at the reducing end together with PMAAs derived from 4-substituted Glc, 2-, 6-substituted Glc and terminal Glc (Figure 3C and D, Supplementary data Figure 3), confirming Glc as the main reducing end saccharide in the unfractionated O-glycan pool.

O-glycan mass spectrometry

In order to obtain more detailed structural information about Mimivirus O-glycans, the β-elimination reaction was performed with $NaBD_4$ as reducing agent. Released glycans were permethylated and per-deuteromethylated, and fragmented by matrix-assisted laser desorption/ionization-mass spectrometry (MALDI-TOF/TOF-MS). The perdeuteromethylation leads to a mass shift relative to the permethylated glycans in accordance with the amount of deuterated methyl groups introduced (Figure 4).

The major O-glycan signals can be referred to sequences with Glc and Vio at the reducing terminus, which is in good agreement with the results obtained from the reducing end analyses (Figure 3B–D). A total of 26 O-glycans were detected and fragment-ion spectra of 15 permethylated and/or perdeuteromethylated oligosaccharides were recorded (Table I).

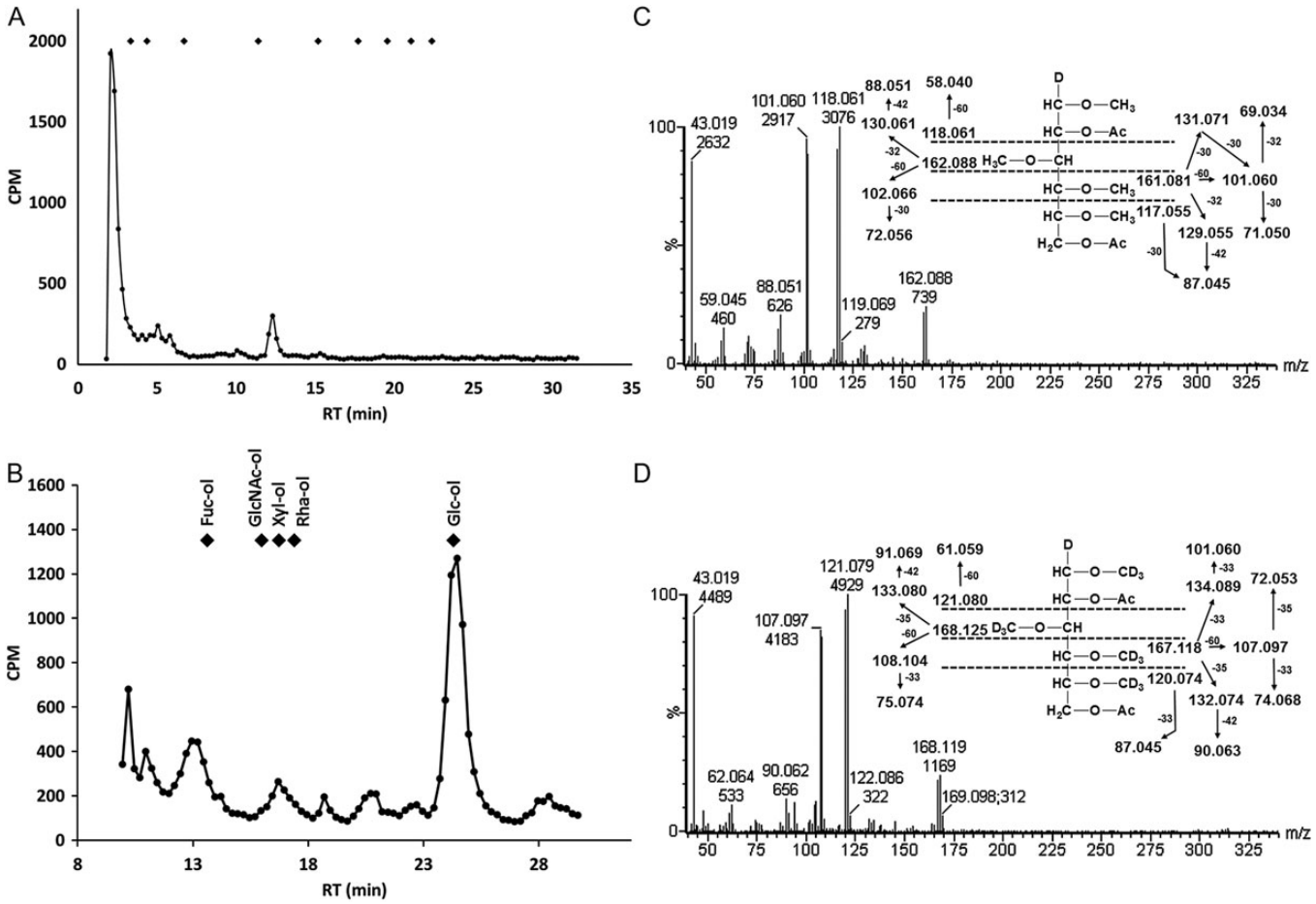

Fig. 3. Mimivirus β-elimination products and reducing end analysis. (**A**) Mimivirus O-glycans were labeled with ^{3}H during the reductive β-elimination reaction and chromatographed by Dionex CarboPac PA200 HPAEC. Fractions were collected and the radioactivity was measured by liquid scintillation counting. Diamonds mark the elution positions of a dextran partial hydrolysate calibrant, starting with a single Glc at the left to a Glc nonamer at the right. (**B**) Radiolabeled O-glycans were acid hydrolyzed, mixed with authentic alditol standards, and chromatographed using a Dionex CarboPac MA1 column coupled to PAD. Alditols were prepared from Fuc (Fuc-ol), GlcNAc (GlcNAc-ol), xylose (Xyl-ol), Rha (Rha-ol), and Glc (Glc-ol). Fractions were collected and the radioactivity was measured by liquid scintillation counting. Diamonds indicate the elution positions of the alditol standards as indicated. The elution profile obtained from the acid hydrolysis of unfractionated O-glycans is shown. (**C**) Electron impact ionization mass spectrum of 1,3,4,5-tetramethyl-2,6-acetyl-glucitol derived from 2-, 6-substituted reducing end Glc of unfractionated Mimivirus O-linked glycans, eluting at the RT of 0.733 relative to 2,3,4,6-trimethyl-1,5-acetyl-glucitol detected by GC–MS. (**D**) Electron impact ionization mass spectrum of 1,3,4,5-tetra-deuteromethyl-2,6-acetyl-glucitol derived from 2-, 6-substituted reducing end Glc of unfractionated Mimivirus O-linked glycans, eluting at the RT of 0.733 relative to 2,3,4,6-tri-deuteromethyl-1,5-acetyl-glucitol detected by GC-MS.

All precursor ions, except for glycan O1.5, were detected in the permethylated as well as in the perdeuteromethylated samples. Furthermore, the use of methyl- and deuteromethyl derivatization was beneficial in detecting methyl- substitutions on Mimivirus glycans, and was supportive in the oligosaccharide sequence determinations. For example, diagnostic fragment ions assigned from spectra of permethylated samples could be confirmed with the corresponding spectra acquired from perdeuteromethylated glycans, providing additional confidence in the glycan sequence assignments. For six O-glycans, fragment ion spectra were recorded from permethylated, as well as perdeuteromethylated samples, allowing identical fragment ion assignments from each sample (Figure 5). Ring fragment analysis was used in saccharide linkage assignments (Supplementary data Table II and Supplementary data Figure 1). Overall, the detected Mimivirus glycans can be divided into six structural groups. All groups, except glycans O1.4 to O1.7, are linear sequences elongated by hexose polymers (Figure 6, Table I).

The Mimivirus glycans O1.4 to O1.7 showed branched conformations with methyl modifications at terminal HexNAc residues and hexose at the reducing end. The hexose residue corresponded to 2-, 6-substituted glucitol as determined by the reducing end analysis (Figure 3B–D). Ring fragment analysis in the spectrum of glycan O1.6 (Figure 6A, Table I, Supplementary data Table II and Supplementary data Figure 1) indicated the presence of terminal pentose in 3- or 4-linkage to HexNAc. The linear glycans can be grouped according to their reducing end residues being di-methylated deoxy-hexose (Me2dHex), methylated deoxy-hexosamine (MedHexN), di-methylated hexose (Me2Hex), hexose (Hex) and methylated hexosamine (MeHexN, Table I).

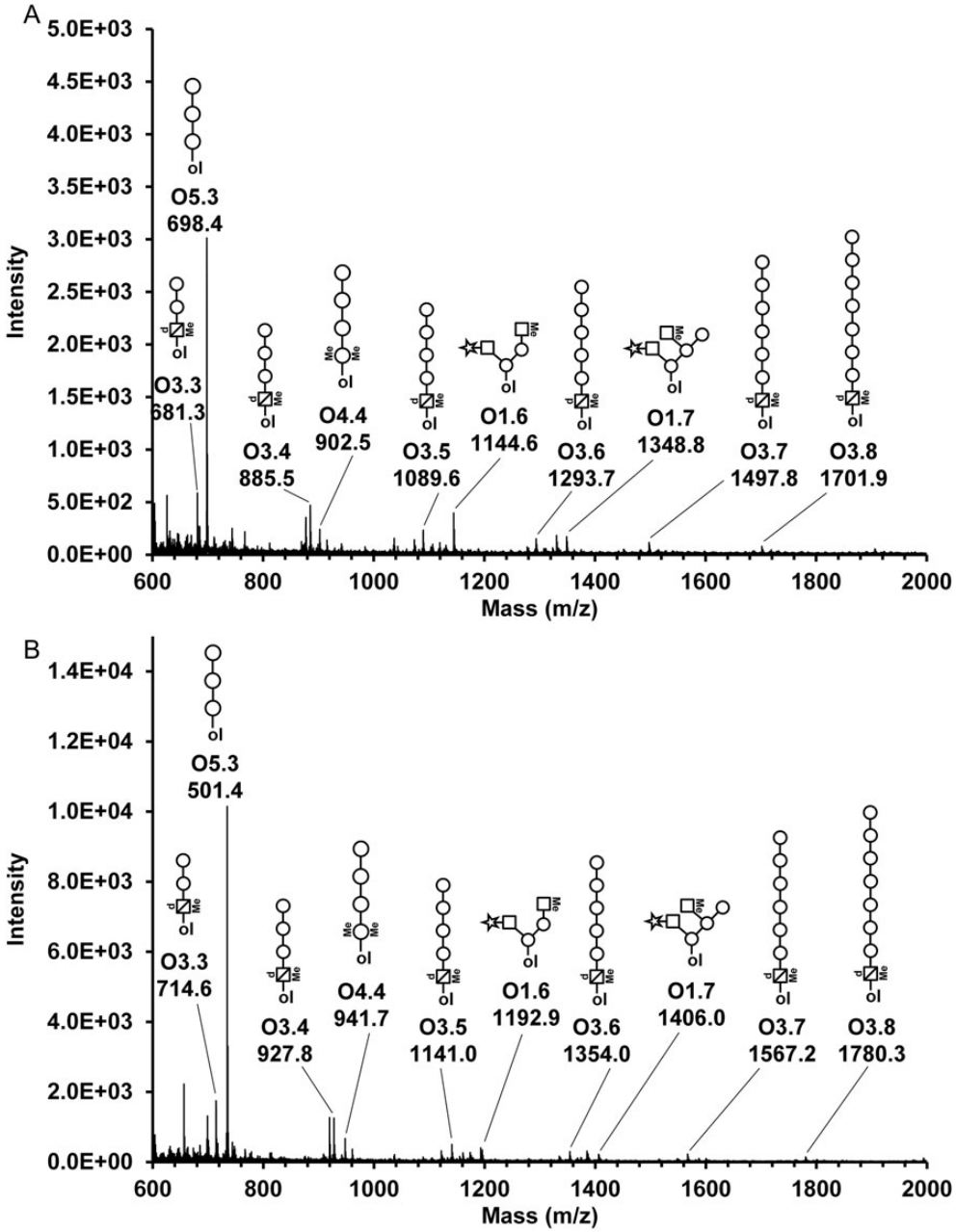

Fig. 4. MALDI-TOF-MS of β-eliminated Mimivirus O-glycans. Mimivirus O-glycans were β-eliminated, permethylated (**A**) or perdeuteromethylated (**B**) and subjected to MALDI-TOF-MS. The molecular ions of major O-glycans are mass annotated and labeled with their corresponding glycan identifications (see Table I). Symbols represent the proposed assignments. Circle, hexose; star, pentose; square, *N*-acetyl-hexosamine; triangle, deoxy-hexose; square with cross-line, hexosamine; d, deoxy; Me, methyl; ol, reducing end.

Combining the results from the MALDI-TOF/TOF-MS fragment ion spectra, the reducing end analysis, the monosaccharide analysis and published data on Mimivirus glycosylation (Piacente et al. 2012), the monosaccharides Me2dHex, MedHexN, Me2Hex, Hex and MeHexN probably correspond to di-methyl-Rha, methyl-Vio, di-methyl-Glc, Glc and methyl-GlcN. The terminal pentose is predicted to be xylose and the oligohexoses to be glucose polymers. Alpha- and beta-anomeric Glc extensions might be present in the hexose-elongated Mimivirus O-glycans, since an altered surface accessibility for biotinylation reagents was observed upon amylase treatment of Mimivirus particles (Supplementary data Figure 2). For the glycans O6.3 to O6.5, the ring fragment analyses suggested glycosidic bonds in 4-linkage to the adjacent hexoses (Table I, Supplementary data Table II and Supplementary data Figure 1). The 4-linkage might also be present in glycans O2.4, O2.5, O3.3, O3.4, O4.4, O4.5 and the terminal residues in O5.4. Nevertheless, the fragment ion spectra corresponding to these saccharides did not indicate ring

Table I. Mimivirus O-glycan sequences

Ident.	Glycan composition	$M+Na^+$ deutero-methylated (measured)	$M+Na^+$ deutero-methylated (calculated)	$M+Na^+$ methylated (measured)	$M+Na^+$ methylated (calculated)	MS2−spectra	Proposed Sequence	Red.-end*
O1.4	HexNAc2Hex2	1029.82	1029.8	984.58	984.52	CH_3	HexNAc-Hex-[HexNAc]-Hex-ol	Glc
O1.5	HexNac2Hex3	n.d.	1242.96	1188.66	1188.62			
O1.6	HexNAcMeHexNAcHex2Pen	1192.89	1192.89	1144.64	1144.59	CH_3/CD_3	MeHexNAc-Hex-[Pen-(3/4)HexNAc]-Hex-ol	Glc
O1.7	HexNAcMeHexNAcHex3Pen	1406.04	1406.05	1348.78	1348.69	CH_3/CD_3	[MeHexNAc-[Hex]-Hex]-[Pen-HexNAc]-Hex-ol	Glc
O2.3	Hex2Me2dHex	695.51	695.52	n.d.	668.36			Me2Rha
O2.4	Hex3Me2dHex	908.69	908.67	n.d.	872.46	CD_3	Hex-(4/6)Hex-Hex-Me2dHex-ol	Me2Rha
O2.5	Hex4Me2dHex	1121.86	1121.83	n.d.	1076.56	CD_3	Hex-(3/4)Hex-Hex-Hex-Me2dHex-ol	Me2Rha
O3.2	HexMedHexN	501.43	501.44	n.d.	477.29	CD_3	Hex-MeVio-ol	MeVio
O3.3	Hex2MedHexN	714.63	714.6	681.33	681.39	CD_3	Hex-(4/6)Hex-MeVio-ol	MeVio
O3.4	Hex3MedHexN	927.8	927.75	885.45	885.49	CD_3	Hex-(4/6)Hex-(4/6)Hex-MeVio-ol	MeVio
O3.5	Hex4MedHexN	1140.97	1140.91	1089.57	1089.59		Hex-Hex-Hex-Hex-MeVio-ol	MeVio
O3.6	Hex5MedHexN	1354.04	1354.07	1293.68	1293.69		Hex-Hex-Hex-Hex-Hex-MeVio-ol	MeVio
O3.7	Hex6MedHexN	1567.2	1567.22	1497.79	1497.79		Hex-Hex-Hex-Hex-Hex-Hex-MeVio-ol	MeVio
O3.8	Hex7MedHexN	1780.34	1780.38	1701.9	1701.89		Hex-Hex-Hex-Hex-Hex-Hex-Hex-MeVio-ol	MeVio
O3.9	Hex8MedHexN	1993.54	1993.53	1906.03	1905.99		Hex-Hex-Hex-Hex-Hex-Hex-Hex-Hex-MeVio-ol	MeVio
O3.10	Hex9MedHexN	2206.68	2206.69	2110.14	2110.09		Hex-Hex-Hex-Hex-Hex-Hex-Hex-Hex-Hex-MeVio-ol	MeVio
O3.11	Hex10MedHexN	2419.75	2419.85	2314.24	2314.19		Hex-Hex-Hex-Hex-Hex-Hex-Hex-Hex-Hex-Hex-MeVio-ol	MeVio
O3.12	Hex11MedHexN	2632.9	2633	2518.32	2518.29		Hex-Hex-Hex-Hex-Hex-Hex-Hex-Hex-Hex-Hex-Hex-MeVio-ol	MeVio
O4.3	Hex2Me2Hex	728.55	728.56	698.37	698.37		Hex-Hex-Me2Hex-ol	Me2Glc
O4.4	Hex3Me2Hex	941.73	941.71	n.d.	902.47	CD_3	Hex-(3/4)Hex-(4/6)Hex-Me2Hex-ol	Me2Glc
O4.5	Hex4Me2Hex	1154.87	1154.87	1106.6	1106.57	CD_3	Hex-(3/4)Hex-Hex-(3/4)Hex-Me2Hex-ol	Me2Glc
O5.3	Hex3	734.63	734.59	698.37	698.37	CH_3/CD_3	Hex-(4)Hex-Hex-ol	Glc
O5.4	Hex4	947.81	947.75	902.48	902.47	CH_3/CD_3	Hex-(4/6)Hex-(4)Hex-Hex-ol	Glc
O6.3	Hex2MeHexN	747.6	747.63	711.34	711.4	CH_3	Hex-(4)Hex-MeHexN-ol	MeGlcN
O6.4	Hex3MeHexN	960.76	960.78	915.47	915.5	CH_3/CD_3	Hex-(4)Hex-(4)Hex-MeHexN-ol	MeGlcN
O6.5	Hex4MeHexN	1173.93	1173.94	1119.59	1119.6	CH_3/CD_3	Hex-(4)Hex-(4)Hex-(4)Hex-MeHexNol	MeGlcN

*Reducing end assignment is based on the reducing-end analyses, monosaccharide analysis and published data on Mimivirus glycosylation (Piacente et al. 2012). O-glycan sequence assignments were supported by fragment ion recordings and most confident sequence information were obtained from identical fragment ion assignments inferred from permethylated and perdeuteromethylated glycan samples (MS2 spectra, CH_3/CD_3). Mass annotated MS2-spectra are shown in Supplementary data Figure 1 and the assigned fragment ions are listed in Supplementary data Table II. Individual glycans are named with O1 to O6 referring to the glycan grouping applied, whereas the second digits correspond to the number of residues or the size of the O-glycan.

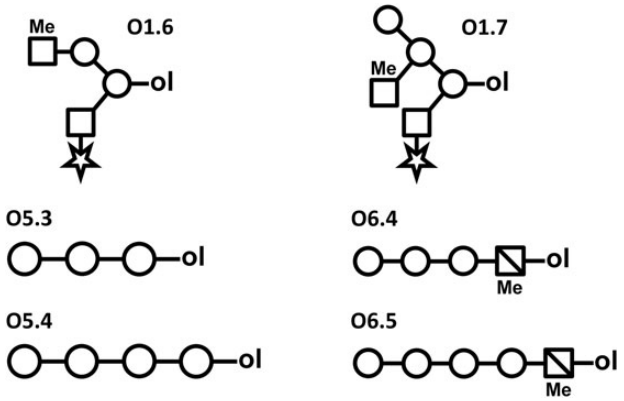

Fig. 5. Schematic representation of selected Mimivirus O-glycans. For glycans O1.6, O1.7, O5.3, O5.4, O6.4 and O6.5 precursor ion signals and fragment ion spectra were recorded from permethylated and perdeuteromethylated samples, allowing for high confidence sequence assignments. Circle, hexose; star, pentose; square, *N*-acetyl-hexosamine; square with cross line, hexosamine; Me, methyl; ol, reducing end.

fragmentation solely supportive for 4-linkages (Supplementary data Table II and Supplementary data Figure 1). The detection of PMAA derived from 4-substituted Glc of the unfractionated O-glycans by GC-MS, however, confirms 4-linked internal Glc residues as a major structural motif in Mimivirus O-glycans (Supplementary data Figure 3). Due to the lack of authentic methylated monosaccharide standards, it was not possible to use HPAEC-PAD to confirm the MALDI-TOF-MS data suggesting that mono- and di-methylated monosaccharides are at the reducing ends of the O-linked oligosaccharide. Therefore, only the reducing ends for glycans O1.4, O1.6, O1.7, O5.3 and O5.4 could be directly confirmed with the detection of glucitol by HPAEC-PAD. For the O1.4, O1.6 and O1.7 glycans 2-, 6-substituted Glc at the reducing end and at the internal branching residue was indicated by GC-MS analyses of PMAAs derived from the unfractionated glycan pool (Figure 3C and D, Supplementary data Figure 3). Saccharides with Glc at the reducing end constitute the most abundant O-glycans in Mimivirus (Table I, Figures 3B–D and 4) and the branched O-glycans appear to account for a major portion of these glycans, since mono-substituted Glc or other reducing end saccharides could not be identified by GC-MS of PMAAs derived from unfractionated Mimivirus O-glycans. The monosaccharide analysis showed that N-acetylglucosamine (GlcNAc) or GlcN is a major constituent in Mimivirus protein extracts. Although it is the major monosaccharide in the analysis, it does not necessarily imply that GlcNAc is a main constituent in elongated Mimivirus O-glycosylation. GlcNAc may have other functions in Mimivirus or be part of other classes of glycans, apart from O-glycosylation on Ser or Thr.

Effect of amylase treatment on virus infectivity

Next, we addressed the functional significance of Glc elongations of Mimivirus O-glycans on the infectivity toward the

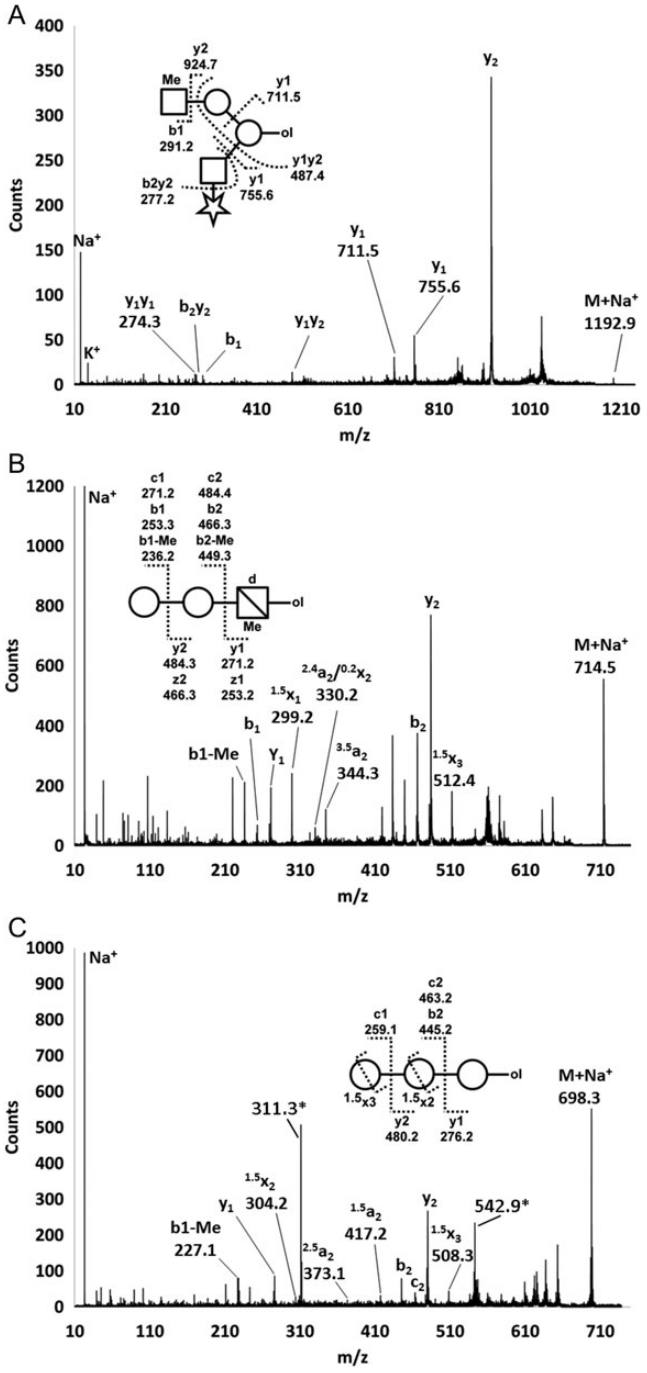

Fig. 6. MALDI-TOF/TOF-MS of permethylated O-glycans. Representative fragment ion spectra of Mimivirus O-glycans. Glycans were β-eliminated from Mimivirus proteins, permethylated and analyzed by MALDI-TOF/TOF-MS. The inserted symbols represent the proposed assignments (**A**) O1.6, perdeuteromethylated, (**B**) O3.3, perdeuteromethylated, (**C**) O5.3, permethylated. Major fragment ions are labeled. Ion masses labeled with "*" could not be assigned to the proposed O-glycan and might originate from MALDI matrix interferences at low precursor ion intensities. Circle, hexose; star, pentose; square, *N*-acetyl-hexosamine; square with cross line, hexosamine; d, deoxy; Me, methyl; ol, reducing end.

amoebal host. *Acanthamoeba polyphaga* was grown to logarithmic phase in 96-well plates and infected with serial dilutions of identical quantities of α-amylase treated and untreated Mimivirus particles. Infected amoebae were assessed with 4′,6-diamidino-2-phenylindole, which results in a distinct fluorescence staining of viral factories in the cytoplasm. The viral titers necessary for infection were shown to be identical in amylase digested and undigested Mimivirus samples, indicating that α-Glc elongations of Mimivirus surface glycans do not play a role in the establishment of infection in the amoebal host (Figure 7).

Discussion

The present study established that O-glycosylation is complex and diverse in Mimivirus. This suggests that Mimivirus O-glycosylation serves equally diverse and complex roles in Mimivirus infection. Several NCLDVs families and Mimiviridae are remarkable in the sense that instead of utilizing or modifying the host glycosylation pathways, they rely on their own glycosylation machinery (Parakkottil et al. 2010; Luther et al. 2011; Piacente et al. 2012). Nevertheless, it remains unanswered why Mimivirus glycosylates its surface proteins. Upon infection of the host, Mimivirus expresses most of its protein coding sequences, indicating that they are likely to be required to perform key life cycle processes. Therefore, the expression of the genome-encoded metabolic and biosynthetic pathways seem to be of advantage for the virus to replicate within the host. The Mimivirus genome repertoire appears to be nearly self-sufficient for replication, since it completes its entire lifecycle exclusively in cytoplasmic viral factory assemblies, superseding the need for initial DNA replication in the nucleus (Mutsafi et al. 2010). In this study we describe O-glycans with methyl and pentose substitutions to hexosamine residues. In Mimivirus, corresponding transferase enzymes have not been identified. On the other hand, terminally methylated and pentosylated N-glycans were also described recently in *Acanthamoeba* spp. (Schiller et al. 2012). It is tempting to speculate that Mimivirus may in part utilize host enzymes for O-glycan biosynthesis. Methylated and pentose substituted N-glycans were also identified in higher eukaryotic organisms, such as in snails (*Helix pomatia*, *Lymnaea stagnalis* and *Biomphalaria glabrata*) as well as in the parasitic worm *Schistosoma mansoni* (van Kuik, van Halbeek et al. 1985; Van Kuik, Sijbesma et al. 1986; Van Kuik, Sijbesma, Kamerling et al. 1987; Geyer et al. 2005; Lehr et al. 2007). On the basis of immunological cross-reactivity and common carbohydrate epitopes found in these organisms, carbohydrate-mediated molecular mimicry involved in host–parasite interactions has been discussed as a possible biological role of such glycan modifications.

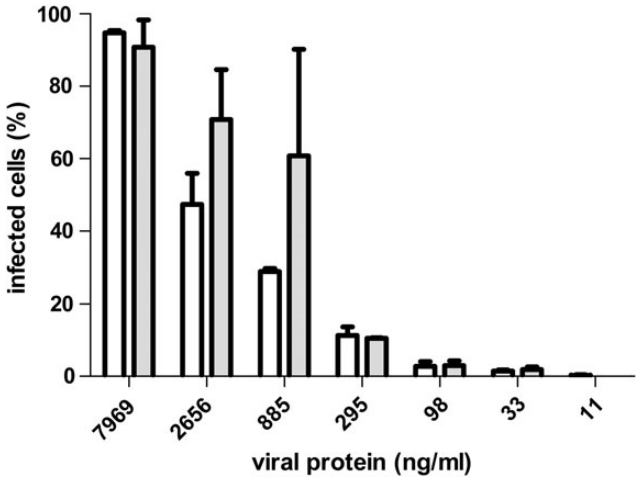

Fig. 7. Mimivirus titer after amylase digestion. Mimivirus particles were treated with α-amylase and added in serial dilutions to *A. polyphaga* grown in 96-well plates. After an incubation of 6 h at 28°C amoeba were stained with 4′,6-diamidino-2-phenylindole in PBS and the number of infected amoeba were counted and plotted against the virus concentration in ng protein per ml. Empty bars show the titer of untreated Mimivirus. Grey bars show the titer of α-amylase digested Mimivirus. Error bars indicate the standard error of mean and were calculated from three infections per virus titer.

The glycosylation in Mimivirus may have a role in facilitating capture by the amoebal host. Mimivirus glycans may be required for host infection via initial binding to *Acanthamoeba*-expressed receptors. We addressed this question by testing the infectivity of Mimivirus after the removal of terminal Glc residues from the virus surface, and were unable to show a difference in infectivity after amylase treatment of virus particles. Therefore, the Glc-elongated O-glycans described here might have other biological functions. In Mimivirus, host-binding epitopes might be represented by different glycoforms or surface structures. *Acanthamoeba* express Man-binding lectins, which mediate adhesion to the mammalian host during establishment of infection resulting in a cytopathic effect. Man-binding lectin-mediated interactions are thought to play a role in the amoeba-induced cytopathic effect by triggering the secretion of contact-dependent cytotoxic proteases (Panjwani 2010). Other functional roles for lectins in amoebae were described in the human pathogen *Entamoeba histolytica* and the free living social amoeba *Dictyostelium discoideum. Entamoeba histolytica* expresses a trimeric Gal and N-acetylgalactosamine (GalNAc)-binding lectin, which plays an essential role in cell adherence and cytotoxicity. In this case, the Gal/GalNAc-lectin also mediates evasion of the host complement system, possibly via molecular mimicry of human CD59 (Petri et al. 2002). On the other hand, *Dictyostelium* discoideum expresses two GalNAc-binding lectins, discoidin I and discoidin II. The precise function of discoidin I and discoidin II is unclear. They may be involved in intercellular adhesion during formation of the spores producing the multicellular fruiting body (Rosen et al. 1973; Frazier et al. 1975).

Mimivirus surface glycosylation may also have a role after uptake by the amoebal host, similar to strategies developed by *Mycobacterium tuberculosis* for establishing infection in the host cell. *Mycobacterium tuberculosis* is taken up by human macrophages via phagocytosis and establishes infection by interfering with phagosomal maturation to lysosomes. It was shown that the man-capped glycosyl-phosphatidylinositol lipoarabinomannan blocks the phosphatidyl-inositol-3-phosphate dependent delivery of cargo from the *trans*-Golgi-network to the phagosome, inducing phagosome maturation arrest (Fratti et al. 2003). Mimivirus was also reported to be phagocytosed by macrophages and virus

uptake was shown to be reduced upon treatment of the cells with a phosphatidylinositol-3-kinase-specific inhibitor. Therefore, it may be conceivable that Mimivirus glycans serve a similar function when taken up by phagocytosis.

The findings described in this study present a basis for further investigations on the biological significance of Mimivirus glycosylation. Structural and topological information on Mimivirus glycosylation will facilitate studies on the mechanisms for establishing infection in the amoebal host. Furthermore, the information provided in this study will be beneficial for further characterization of glycosyltransferases in Mimivirus, aiding future investigations on the functional significance of Mimivirus glycosylation.

Materials and methods

Periodate oxidation and amino-oxy-biotinylation of Mimivirus surface glycoproteins

For biotinylation of periodate oxidized surface glycoproteins, we adapted a method described earlier based on amino-oxy-biotinylation of sialo-glycoproteins on living cells (Dirksen et al. 2006; Zeng et al. 2009). Mimivirus was grown on *Acanthamoeba polyphaga* cultured in PYG medium as described (Shah et al. 2014). After 2 days, viral particles were collected from the amoeba lysates and purified by filtration through a 0.8 µm membrane, followed by centrifugation at 6000 × g. The Mimivirus pellet was washed at least six times with PBS and resuspended to 450 µL with ammonium acetate-buffered saline (100 mM ammonium acetate, 150 mM NaCl). A 100 mM Na-meta-periodate solution was prepared freshly with ammonium acetate-buffered saline and 50 µL was added to the Mimivirus sample, resulting in a final concentration of 10 mM Na-meta-periodate for the oxidation of glycans. Blank samples were prepared by adding 50 µL ammonium acetate-buffered saline only. The samples were incubated for 30 min at room temperature, in the dark and an equal volume freshly prepared 10 mM Na-meta-periodate in ammonium acetate-buffered saline was added. Incubation was continued for further 30 min at room temperature, in the dark. The reaction was quenched by adding 10 µL of 100 mM glycerol in ammonium acetate-buffered saline each, followed by two washes with ammonium acetate-buffered saline. The Periodate-oxidized samples were resuspended in 1 mL 10 mM aniline and amino-oxy-biotin (Biotium Inc.) was added to give a final concentration of 0.1 mM. The samples were incubated for 90 min at 4°C followed by two washes with 0.5 mL of ammonium acetate-buffered saline and subjected to protein extraction. Proteins were extracted by adding extraction buffer (0.5 M Tris–HCl, pH 8.5, 0.2% CHAPS detergent, 5 mM TCEP, containing 100 mg GuHCl per 150 µL buffer) and incubated at 60° C for 1 h. Samples were cooled to room temperature and free sulfhydryl groups were alkylated by adding 2 µmol methyl methanethiosulfonate (MMTS). The extract was diluted 10-fold with PBS, 0.1% CHAPS, containing proteinase inhibitors (Calbiochem Proteinase Inhibitor Cocktail III, Merck Millipore, USA) and subjected to an avidin cartridge purification (AB Sciex, USA). The sample was applied to the avidin cartridge, equilibrated with PBS, 0.1% CHAPS. The cartridge was washed with 500 µL PBS, 0.1% CHAPS, 1 mL 650 mM NaCl in 20 mM phosphate buffer, pH 7.2, 0.1% CHAPS, 1 mL PBS, 0.1% CHAPS, 1 mL 0.1% CHAPS in H_2O successively and biotinylated Mimivirus proteins were eluted with 800 µL 0.4% TFA, 0.1% CHAPS. The proteins were precipitated using TCA. Nonoxidized blank samples were processed in parallel to oxidized samples and digested with 0.2 µg Lys-C in 0.5 M triethylammonium bicarbonate buffer, pH 8.5, 0.1% sodium dodecyl sulfate, for 2 h at 37°C, followed by adding 5 µg trypsin to give a final volume of 30 µL. The samples were digested at 37°C for 16 h. Oxidized versus blank samples were differentially labeled with the 4-plex iTRAQ labeling kit and subjected to cation exchange cartridge purification (AB Sciex, USA), following the manufacturer's instructions. Samples were desalted using ZipTip C18 tips (Millipore, USA) prior to LC-MS on an Orbitrap XL mass spectrometer (ThermoFischer Scientific Inc., USA), coupled to an Eksigent nano LC system (Eksigent Technologies, USA).

Peptides were separated on a capillary tip column (75 µm × 80 mm) packed with reverse phase C18 material (AQ, 3 µm 200 Å, Bischoff GmbH, Germany). The column was equilibrated with 95% solvent A (1% acetonitrile; 0.2% formic acid in water) and 5% solvent B (80% acetonitrile; 0.2% formic acid in water). Peptides were eluted with a flow rate of 200 nL/min using a 55 min linear gradient from 3 to 57% solvent B. The analyses were performed in the data-dependent acquisition mode. The three most intense precursor ions in the mass range *m/z* 300–2000 were selected and one CID and a HCD spectrum were acquired per precursor ion. Nominal collision energies of 35 and 42 V were applied for CID and HCD, respectively. Dynamic exclusion was switched on, ensuring that up to 500 *m/z* ratios ±20 ppm values were excluded from MS/MS for 90 s. The instrument was calibrated externally according to the manufacturer's instructions.

The iTRAQ reporter ion channels from the HCD spectra were concatenated to the CID fragment ion spectra *in silico* and analyzed using the Mascot search algorithm (Matrix Science, UK; Version: 2.4.1). Mascot was set up to search the Swissprot database (downloaded 11.01.2011, 1,049,100 entries, containing decoy dataset and common contaminants) assuming the digestion enzyme trypsin with maximal one missed cleavage. Mascot was searched with a fragment ion mass tolerance of 0.60 Da and a parent ion tolerance of 10.0 ppm. MMTS alkylation of cysteine and AB Sciex iTRAQ multiplexed quantitation chemistry of lysine and the N-terminus were specified in Mascot as fixed modifications. Oxidation of methionine and AB Sciex iTRAQ multiplexed quantitation chemistry of tyrosine were specified in Mascot as variable modifications. Scaffold (version Scaffold_3.4.9, Proteome Software Inc., USA) was used to validate MS/MS-based peptide and protein identifications. Peptide identifications were accepted if they could be established at >80.0% probability as specified by the Peptide Prophet algorithm (Keller et al. 2002). Protein identifications were accepted if they could be established at greater than 99.0% probability and contained at least two identified peptides. Protein probabilities were assigned by the Protein Prophet algorithm (Nesvizhskii et al. 2003). Additionally, peptide fragmentation spectra were manually inspected for sequence identification and iTRAQ reporter ion generation. The Q+ multiplex calculation browser within Scaffold was

used for quantification of the iTRAQ results, separately in pairs of avidin-enriched sample and blank sample. Individual quantitative samples were normalized within each acquisition run. Intensities for each peptide identification were normalized within the assigned protein. The intensity-based, median-type normalization and the average protein reference option with normalization between samples were used. Nonunique peptides were excluded from the calculations. Reporter ion peak heights above 1% of the highest peak in a spectrum were used for quantitation. The quantitation results expressed as $\log_2$ of the fold enrichment were exported from Scaffold and analyzed in Microsoft-Excel 2010. To assess the significance for a particular protein being enriched when biotinylated, we calculated the mean values for enrichment above 0 using Student's *t*-test. We assumed that binding of nonbiotinylated and biotinylated proteins to the avidin cartridge is normal distributed, with equal variances for both groups. The *t*-values were calculated by dividing the mean by the standard error ($standard\ deviation/\sqrt[2]{n}$) and the degree of freedom values were determined ($df = n - 1$). The T.DIST function in MS-Excel was used to determine the significance level values with the cumulative distribution function.

Monosaccharide analysis

Mimivirus protein extracts were pre-mixed with Gal as internal standard and hydrolyzed with 2 M TFA for 4 h at 100°C. The hydrolyzate was dried, re-dissolved in water and subjected to monosaccharide analysis using a CarboPac PA20 column attached to a HPAEC-PAD (Dionex, ThermoFischer, USA). For quantitation, an external standard containing Rha, GlcNAc, Gal and Glc was used. For analytical purposes, Vio, Fuc, arabinose, GalNAc, xylose and Man were used as standards.

Structural analysis of Mimivirus O-glycosides

Mimivirus O-glycans were liberated from protein extracts by β-elimination in 0.1 M NaOH, 1 M $NaBD_4$, for 72 h at 37°C essentially as described previously (Hülsmeier et al. 2011). Additionally, released glycans were purified using a paper-disk-column. Paper disks were punched from Whatman 3MM paper using an office-type hole puncher. About 20 paper disks were placed in a centrifugal filter device (Ultrafree-MC, 0.45 µm, Millipore, USA), washed with water and equilibrated with butanol:ethanol:water (4:1:1, v:v:v). The β-elimination products were dissolved in 300 µL water, 300 µL ice-cold ethanol and 1200 µL ice-cold butanol were added, and the sample was loaded onto the paper disks by centrifugation at 100 × *g*. The paper disk cartridge was washed with 2.5 mL of butanol:ethanol:water (4:1:1, v:v:v) and the O-glycans were eluted with 2 mL water by centrifugation at 300 × *g*. The eluate was dried and subjected to permethylation or perdeuteromethylation using the NaOH method (Hülsmeier et al. 2011). Permethylated glycans were dissolved in 10% acetonitrile and applied to a SepPak C18 cartridge (Waters, USA), equilibrated with 10% acetonitrile. The SepPak cartridge was washed with 4.5 mL of 15% acetonitrile and the glycans were eluted with 6 mL of 80% acetonitrile and analysed by MALDI-TOF/TOF-MS (Hülsmeier et al. 2011). MS–MS spectra were acquired with an ABSciex MALDI-TO/TOF 5800 mass spectrometer using the instrument parameters as described earlier (Hülsmeier et al. 2010). Fragment ions were annotated aided by the GlycoWorkbench software, version 2.1 (Ceroni et al. 2008).

O-glycan reducing end analysis

O-glycans were radiolabelled during the β-elimination reaction by incubating Mimivirus protein extract in 0.1 mL of 0.1 M NaOH, 1 M $NaBD_4$, 5 mCi NaB^3H_4 (15 Ci/mmol, Hartmann Analytic GmbH, Germany), for 72 h at 37°C and processed as described (Hülsmeier et al. 2011). Radiolabeled O-glycans were chromatographed by HPAEC, using a CarboPac PA200 column (Dionex, ThermoFischer, USA). The column was equilibrated in 0.1 M NaOH and 5 min after injecting the samples a linear gradient from 0.1 M NaOH to 0.1 M NaOH, 0.15 M sodium acetate, over 40 min at 0.4 mL/min was applied. Fractions were collected every 15 s and 1/10 volume per fraction was measured by scintillation counting (Packard Tri-Carb 2900TR liquid scintillation counter, PerkinElmer, USA). The column flow through up to 5 min retention time (RT), the eluate between 5 and 7 min and the peak fractions between 41 and 45 min were combined, desalted by passage through a 4.5 mL column of Dowex AG 50 × 8 (BioRad, USA), equilibrated and eluted with water. The combined fractions and an aliquot taken prior to CarboPac PA200 chromatography were subjected to acid hydrolysis with 2 M TFA for 4 h at 100°C. The hydrolysates were dried and resuspended three times from 0.1 mL methanol and mixed with alditol standards, prepared from Fuc, GlcNAc, Xyl, Rha, Glc, 1 nmol each, and 5 nmol inositol. The alditol mixture was chromatographed by HPAEC-PAD, using a CarboPac MA1 column (Dionex, ThermoFischer, USA). The column was equilibrated in 60 mM NaOH and 5 min after injecting the samples a linear gradient from 60 mM NaOH to 660 mM NaOH, over 30 min at 0.4 mL/min was applied. Fractions were collected directly into scintillation vials every 15 s, neutralized with acetic acid and measured by scintillation counting.

For analyses by GC-MS, unfractionated permethylated and perdeuteromethylated O-glycans were hydrolyzed in 0.5 mL of 4 M TFA for 4 h at 100°C. The samples were dried under a stream of N_2 and reduced over night with 0.5 mL 250 mM $NaBD_4$ in 1 M ammonia at 4°C. The samples were acidified with 20% acetic acid in methanol and dried under a stream of N_2. Borate salts were removed by evaporation twice from 2 mL of 1% acetic acid in methanol followed by three evaporations from 2 mL methanol. Partially methylated alditols were dissolved in 0.8 mL pyridine/acetic anhydride (1:1, v:v) and incubated under argon gas over night at 4°C. The samples were dried under N_2, re-dissolved in 2 mL dichloromethane and subjected to 6–12 washes with 1 mL water each. The samples were dried under N_2, resuspended in 10–100 µL dichloromethane and 1 µL was injected in a GCT Premier gas chromatograph mass spectrometer, using electron impact ionization at 70 eV (Waters Corp., USA). The chromatography was carried out using a 0.25 mm × 30 m Rxi-5Sil MS w/10 m Integra-Guard capillary column (Restek, USA) with an initial helium gas flow of 1 mL/min. The initial oven temperature of 80°C was held for 2 min, increased at 25°C/min until 130°C, followed by an increase of 1.5°C/min until 200°C and 4°C/min until 290°C. The final temperature was held for 10.83 min, resulting in a total run

time of 84 min. MS acquisition was performed by linear scanning from *m/z* 40–840.

Mimivirus particle biotinylation and amylase digestion

Mimivirus particles were digested with α-amylase (500 U, *Bacillus* sp., Sigma, Switzerland), in 1 mL PBS containing Protease Inhibitor Cocktail Set 1 (Calbiochem, Millipore, USA) for 90 min, rotating at room temperature. The particles were washed twice with PBS and subjected to protein biotinylation with sulpho-NHS-biotin (Pierce, USA) followed by protein purification with avidin cartridges as described above. A second Mimivirus particle sample was biotinylated omitting amylase digestion. The purified proteins were digested with trypsin, desalted with ZipTip C18 tips and subjected to LC–MS.

Mimivirus titer measurement

Acanthamoeba polyphaga was grown to logarithmic phase in flat bottom 96-well plates. Identical amounts of Mimivirus particles (2.4 mg protein per mL PBS) were treated or untreated with α-amylase as described above and diluted 1:10 with PBS followed by 12 dilutions of 1:3 in the 96-well plate per infection. Amoebae were incubated for 6 h at 28°C to establish infection. Then, the PYG medium was aspired and surface-attached amoebae were washed with PBS, followed by fixation with 3% paraformaldehyde in PBS for 10 min. Amoebae and viral factories were stained with 0.1 µg per ml 4′,6-diamidino-2-phenylindole (Sigma, USA) in PBS for 15 min, washed with PBS and counted using fluorescence microscopy. Infected cells were assessed as amoebae containing viral factories and plotted against the virus protein per well. The tissue culture infectious dose at 50% per mL was calculated to be 1.022×10^3 and corresponds to 2.9 µg viral protein per mL. Differences in infection with treated versus untreated virus particles were evaluated using the paired, two-tailed Student's *t*-test function with 95% confidence intervals in GraphPad Prism (Version 5.03).

Supplementary Data

Supplementary data for this article is available online at http://glycob.oxfordjournals.org/.

Funding

This work was supported by the Swiss National Science Foundation (grant number: 310030-129633) to T.H. and the Stiftung für wissenschaftliche Forschung an der Universität Zürich to A.J.H and T.H.

Acknowledgements

We thank Professor Michela Tonetti, University of Genova, Italy, for providing the Vio standard. We a grateful to Drs Peter Gehrig, Bernd Roschitzki, Jonas Grossmann, Endre Laczko and Tshering Altherr at the Functional Genomics Center Zurich for their support with the mass spectrometric analyses.

Abbreviations

Fuc, fucose; Gal, galactose; GalNAc, N-acetylgalactosamine; GC–MS, gas chromatography mass spectrometry; Glc, glucose; GlcN, glucosamine; GlcNAc, N-acetylglucosamine; Hex, hexose; HexNAc; HPAEC, high performance anion exchange chromatography; HPAEC-PAD, high performance anion exchange chromatography with pulsed amperometric detection; MALDI-MS or MALDI-TOF/TOF-MS, matrix-assisted laser desorption/ionization-mass spectrometry.; Man, mannose; Me2dHex, di-methylated deoxy-hexose; MedHexN, methylated deoxy-hexosamine; MeHexN, methylated hexosamine; MMTS, methyl methanethiosulfonate; NCLDV, nucleocytoplasmic large DNA viruses; PAGE, polyacrylamide gel electrophoresis; PBS, phosphate-buffered saline; PMAAs, perdeuteromethylated alditol acetates; Rha, rhamnose; RT, retention time; Vio, viosamine.

References

Boughalmi M, Saadi H, Pagnier I, Colson P, Fournous G, Raoult D, La Scola B. 2013. High-throughput isolation of giant viruses of the Mimiviridae and Marseilleviridae families in the Tunisian environment. *Environ Microbiol*. 15:2000–2007.

Boyer M, Azza S, Barrassi L, Klose T, Campocasso A, Pagnier I, Fournous G, Borg A, Robert C, Zhang X, et al. 2011. Mimivirus shows dramatic genome reduction after intraamoebal culture. *Proc Natl Acad Sci USA*. 108:10296–10301.

Ceroni A, Maass K, Geyer H, Geyer R, Dell A, Haslam SM. 2008. GlycoWorkbench: A tool for the computer-assisted annotation of mass spectra of glycans. *J Proteome Res*. 7:1650–1659.

Claverie JM, Abergel C. 2009. Mimivirus and its virophage. *Annu Rev Genet*. 43:49–66.

De Castro C, Molinaro A, Piacente F, Gurnon JR, Sturiale L, Palmigiano A, Lanzetta R, Parrilli M, Garozzo D, Tonetti MG, et al. 2013. Structure of N-linked oligosaccharides attached to chlorovirus PBCV-1 major capsid protein reveals unusual class of complex N-glycans. *Proc Natl Acad Sci USA*. 110:13956–13960.

Dirksen A, Hackeng TM, Dawson PE. 2006. Nucleophilic catalysis of oxime ligation. *Angew Chem Int Ed Engl*. 45:7581–7584.

Fratti RA, Chua J, Vergne I, Deretic V. 2003. Mycobacterium tuberculosis glycosylated phosphatidylinositol causes phagosome maturation arrest. *Proc Natl Acad Sci USA*. 100:5437–5442.

Frazier WA, Rosen SD, Reitherman RW, Barondes SH. 1975. Purification and comparison of two developmentally regulated lectins from *Dictyostelium discoideum*. Discoidin I and II. *J Biol Chem*. 250:7714–7721.

Geyer H, Wuhrer M, Resemann A, Geyer R. 2005. Identification and characterization of keyhole limpet hemocyanin N-glycans mediating cross-reactivity with *Schistosoma mansoni*. *J Biol Chem*. 280:40731–40748.

Hakim M, Ezerina D, Alon A, Vonshak O, Fass D. 2012. Exploring ORFan domains in giant viruses: Structure of mimivirus sulfhydryl oxidase R596. *PLoS One*. 7:e50649.

Honeyman J, Shaw CJG. 1959. 493. Periodate oxidation. Part IV. The effect of conformation of cyclic glycols on the rate of periodate oxidation. *Journal of the Chemical Society (Resumed)*. 0:2454–2465.

Hülsmeier AJ, Deplazes P, Naem S, Nonaka N, Hennet T, Köhler P. 2010. An Echinococcus multilocularis coproantigen is a surface glycoprotein with unique O-gycosylation. *Glycobiology*. 20:127–135.

Hülsmeier AJ, Welti M, Hennet T. 2011. Glycoprotein maturation and the UPR. *Methods Enzymol*. 491:163–182.

Keller A, Nesvizhskii AI, Kolker E, Aebersold R. 2002. Empirical statistical model to estimate the accuracy of peptide identifications made by MS/MS and database search. *Analytical Chemistry*. 74:5383–5392.

Legendre M, Santini S, Rico A, Abergel C, Claverie JM. 2011. Breaking the 1000-gene barrier for Mimivirus using ultra-deep genome and transcriptome sequencing. *Virol J*. 8:99.

Lehr T, Geyer H, Maass K, Doenhoff MJ, Geyer R. 2007. Structural characterization of N-glycans from the freshwater snail *Biomphalaria glabrata* cross-reacting with *Schistosoma mansoni* glycoconjugates. *Glycobiology*. 17:82–103.

Luther KB, Hülsmeier AJ, Schegg B, Deuber SA, Raoult D, Hennet T. 2011. Mimivirus collagen is modified by bifunctional lysyl hydroxylase and glycosyltransferase enzyme. *J Biol Chem*. 286:43701–43709.

Mutsafi Y, Zauberman N, Sabanay I, Minsky A. 2010. Vaccinia-like cytoplasmic replication of the giant Mimivirus. *Proc Natl Acad Sci USA*. 107:5978–5982.

Nandhagopal N, Simpson AA, Gurnon JR, Yan X, Baker TS, Graves MV, Van Etten JL, Rossmann MG. 2002. The structure and evolution of the major capsid protein of a large, lipid-containing DNA virus. *Proc Natl Acad Sci USA*. 99:14758–14763.

Nesvizhskii AI, Keller A, Kolker E, Aebersold R. 2003. A statistical model for identifying proteins by tandem mass spectrometry. *Analytical Chemistry*. 75:4646–4658.

Panjwani N. 2010. Pathogenesis of acanthamoeba keratitis. *Ocul Surf*. 8:70–79.

Parakkottil Chothi M, Duncan GA, Armirotti A, Abergel C, Gurnon JR, Van Etten JL, Bernardi C, Damonte G, Tonetti M. 2010. Identification of an L-rhamnose synthetic pathway in two nucleocytoplasmic large DNA viruses. *Journal of Virology*. 84:8829–8838.

Petri WA, Jr, Haque R, Mann BJ. 2002. The bittersweet interface of parasite and host: Lectin-carbohydrate interactions during human invasion by the parasite *Entamoeba histolytica*. *Annu Rev Microbiol*. 56:39–64.

Philippe N, Legendre M, Doutre G, Coute Y, Poirot O, Lescot M, Arslan D, Seltzer V, Bertaux L, Bruley C, et al. 2013. Pandoraviruses: Amoeba viruses with genomes up to 2.5 Mb reaching that of parasitic eukaryotes. *Science*. 341:281–286.

Piacente F, Marin M, Molinaro A, De Castro C, Seltzer V, Salis A, Damonte G, Bernardi C, Claverie JM, Abergel C, et al. 2012. Giant DNA virus mimivirus encodes pathway for biosynthesis of unusual sugar 4-amino-4,6-dideoxy-D-glucose (Viosamine). *J Biol Chem*. 287:3009–3018.

Raoult D, Audic S, Robert C, Abergel C, Renesto P, Ogata H, La Scola B, Suzan M, Claverie JM. 2004. The 1.2-megabase genome sequence of Mimivirus. *Science*. 306:1344–1350.

Renesto P, Abergel C, Decloquement P, Moinier D, Azza S, Ogata H, Fourquet P, Gorvel JP, Claverie JM. 2006. Mimivirus giant particles incorporate a large fraction of anonymous and unique gene products. *J Virol*. 80:11678–11685.

Rosen SD, Kafka JA, Simpson DL, Barondes SH. 1973. Developmentally regulated, carbohydrate-binding protein in *Dictyostelium discoideum*. *Proc Natl Acad Sci USA*. 70:2554–2557.

Schiller B, Makrypidi G, Razzazi-Fazeli E, Paschinger K, Walochnik J, Wilson IB. 2012. Exploring the unique N-glycome of the opportunistic human pathogen Acanthamoeba. *J Biol Chem*. 287:43191–43204.

Shah N, Hülsmeier AJ, Hochhold N, Neidhart M, Gay S, Hennet T. 2014. Exposure to mimivirus collagen promotes arthritis. *Journal of Virology*. 88:838–845.

Thomas V, Bertelli C, Collyn F, Casson N, Telenti A, Goesmann A, Croxatto A, Greub G. 2011. Lausannevirus, a giant amoebal virus encoding histone doublets. *Environ Microbiol*. 13:1454–1466.

Van Etten JL, Gurnon JR, Yanai-Balser GM, Dunigan DD, Graves MV. 2010. Chlorella viruses encode most, if not all, of the machinery to glycosylate their glycoproteins independent of the endoplasmic reticulum and Golgi. *Biochim Biophys Acta*. 1800:152–159.

Van Etten JL, Lane LC, Dunigan DD. 2010. DNA viruses: The really big ones (giruses). *Annu Rev Microbiol*. 64:83–99.

Van Kuik JA, Sijbesma RP, Kamerling JP, Vliegenthart JF, Wood EJ. 1986. Primary structure of a low-molecular-mass N-linked oligosaccharide from hemocyanin of Lymnaea stagnalis. 3-O-methyl-D-mannose as a constituent of the xylose-containing core structure in an animal glycoprotein. *Eur J Biochem*. 160:621–625.

Van Kuik JA, Sijbesma RP, Kamerling JP, Vliegenthart JF, Wood EJ. 1987. Primary structure determination of seven novel N-linked carbohydrate chains derived from hemocyanin of *Lymnaea stagnalis*. 3-O-methyl-D-galactose and N-acetyl-D-galactosamine as constituents of xylose-containing N-linked oligosaccharides in an animal glycoprotein. *Eur J Biochem*. 169:399–411.

van Kuik JA, van Halbeek H, Kamerling JP, Vliegenthart JF. 1985. Primary structure of the low-molecular-weight carbohydrate chains of *Helix pomatia* alpha-hemocyanin. Xylose as a constituent of N-linked oligosaccharides in an animal glycoprotein. *J Biol Chem*. 260:13984–13988.

Wilson WH, Van Etten JL, Allen MJ. 2009. The Phycodnaviridae: The story of how tiny giants rule the world. *Curr Top Microbiol Immunol*. 328:1–42.

Xiao C, Chipman PR, Battisti AJ, Bowman VD, Renesto P, Raoult D, Rossmann MG. 2005. Cryo-electron microscopy of the giant Mimivirus. *J Mol Biol*. 353:493–496.

Yan X, Olson NH, Van Etten JL, Bergoin M, Rossmann MG, Baker TS. 2000. Structure and assembly of large lipid-containing dsDNA viruses. *Nat Struct Biol*. 7:101–103.

Zeng Y, Ramya TN, Dirksen A, Dawson PE, Paulson JC. 2009. High-efficiency labeling of sialylated glycoproteins on living cells. *Nat Methods*. 6:207–209.